Title: Combining Polyethylene and Polypropylene: Enhanced Performance with PE/*i*PP Multiblock Polymers

Authors: James M. Eagan[1], Jun Xu[2], Rocco Di Girolamo[1†], Christopher M. Thurber[2], Christopher W. Macosko[2], Anne M. LaPointe[1]*, Frank S. Bates[2]*, Geoffrey W. Coates[1]*

Affiliations:

[1]Department of Chemistry and Chemical Biology, Baker Laboratory, Cornell University, Ithaca, New York 14853, United States.

[2]Department of Chemical Engineering and Materials Science, University of Minnesota, Minneapolis, Minnesota 55455, United States.

[†]Current address: Dipartimento di Scienze Chimiche, Università di Napoli Federico II, Complesso Monte S. Angelo, Via Cintia, I-80126 Napoli, Italy.

*Correspondence to: lapointe@cornell.edu, bates001@umn.edu, coates@cornell.edu

Abstract: Polyethylene (PE) and isotactic polypropylene (*i*PP) comprise nearly two-thirds of the world's plastic. Despite their similar hydrocarbon makeup, the polymers are immiscible with one another. Thus, common grades of PE and *i*PP do not adhere or blend, creating challenges for recycling these materials. We synthesized PE/*i*PP multiblock copolymers using an isoselective alkene polymerization initiator. These polymers can weld common grades of commercial PE and *i*PP together depending on the molecular weights and architecture of the block copolymers. Interfacial compatibilization of phase separated PE and *i*PP with tetrablock copolymer enables morphological control, transforming brittle materials into mechanically tough blends.

One Sentence Summary: Polyethylene/isotactic-polypropylene multiblock copolymers enable welding and composites of the two immiscible polymers.

Main Text: Polyethylene (PE) and isotactic polypropylene (*i*PP) are the two most abundantly produced plastics worldwide. Over 70 million and 50 million metric tons of PE and *i*PP, respectively, are produced annually (*1*). The vast majority of PE and *i*PP are prepared using heterogeneous chromium and titanium catalysts (*2*). Heterogeneous olefin polymerization catalysts have a multitude of active sites, each with their own reactivity differences which give rise to polymers of different molecular weights, molecular weight distributions, and microstructures (*3*). In the case of PE and *i*PP, these differences and their phase separation inhibit interfacial adhesion and erode the mechanical properties of melt blends (*4*). Roughly 5% of the value is retained when these plastics are recycled, typically into lower-value products as a result of sorting expenses and degraded physical properties (*5*). Compatibilizers open opportunities for upcycling recovered PE/*i*PP into equal or higher value materials with lower sorting costs (*6, 7*). Since PE and *i*PP are immensely important economically (ca. > $200 billion in annual sales, worldwide), strategies to combine these materials may have significant potential to impact sustainability and the economy.

Single-site metallocene catalysts have been developed and commercialized to produce polyolefins with a more uniform molecular composition (*8*). These polymers demonstrate distinct physical properties from their heterogeneous counterparts, such as the ability to form interfacial welds (*9*). Many non-metallocene single-site catalysts have also been developed, some

of which demonstrate living character for olefin polymerization as well as precise control over the molecular weight, stereochemistry, and architecture of the resulting polymer (*10, 11*).

Strategies to compatibilize *i*PP and PE all rely on the addition of large amounts (≥10%) of additives, typically amorphous polymers (*12-14*). We became interested in how block copolymers of PE and *i*PP would behave as additives in commercial heterogeneous grade polyolefin materials. Despite the simplicity of this idea, we are aware of only a single example of a well-defined semicrystalline polymer combining blocks of PE and *i*PP. Busico and coworkers used a modified C_2-symmetric zirconium catalyst to synthesize a PE-*b*-*i*PP diblock copolymer (*15, 16*). The *i*PP block was shown to be remarkably stereoregular ($m^4 = 99\%$; $T_m = 151$ °C) and polymerization well controlled ($Đ = 1.3$), but molecular weights were relatively low ($M_n = 22$ kg/mol). Experimental results revealed that the catalyst underwent β-hydride elimination, resulting in limited chain-growth and accessible architectures. As part of our longstanding interest in living olefin polymerization, we sought to develop improved catalysts with longer lifetimes capable of producing higher molecular weight PE/*i*PP diblock and multiblock copolymers.

Pyridylamidohafnium catalysts are active for the high temperature production of high molecular weight *i*PP (*17*) and chain-shuttling polymerization (*18*). We recently described the optimization of a pyridylamidohafnium catalyst (**1**) for the controlled isoselective polymerization of propylene (*19*). We report the use of the catalyst to produce high molecular weight *i*PP-*b*-PE diblock and multiblock copolymers with precise control of block length (Fig. 1).
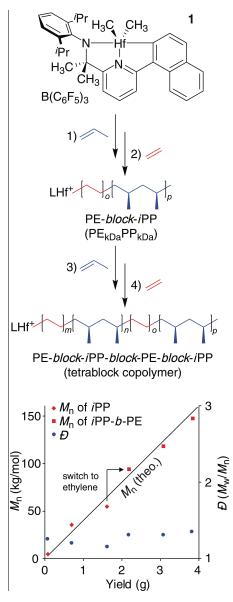
Fig. 1. **Synthesis of PE/*i*PP block copolymers.** The structure of isoselective pyridylamidohafnium catalyst (**1**)/B(C$_6$F$_5$)$_3$ and the controlled polymerization of olefins to ethylene/propylene multiblock copolymers. After quenching with methanol, hafnium end groups were protonated. Molecular weights (M_n) and dispersities ($Đ = M_w/M_n$) were determined using size-exclusion chromatography calibrated with polyethylene standards.

The activation of precatalyst **1** with $B(C_6F_5)_3$ followed by the condensation of propylene into the reaction afforded isotactic polypropylene (Fig. 1). Following complete consumption of propylene, the introduction of ethylene to the reaction vessel resulted in the formation of *i*PP-*b*-PE diblock copolymer. Number average molecular weights (M_n) increased linearly as a function of monomer conversion and were in good agreement with theoretical values, consistent with the behavior of a living polymerization (*20*).

The molecular weight of the ethylene block was controlled by varying reaction time (Table 1, entries 1 and 2) under a constant ethylene feed, while propylene molecular weights were tuned by the monomer/catalyst ratio and full conversion. The single melting endotherms observed (Fig. S2) are due to regio- and stereoerrors in the propylene block, which lower the T_m of the *i*PP homopolymers to 134 °C (vs. ~165 °C for perfect *i*PP) which is very similar to the T_m of the PE block (135 °C). This was confirmed by quantitative ^{13}C NMR spectroscopy (Fig. S1), which showed high stereoselectivity for 1,2-insertion of polypropylene ($m^4 = 91\%$), regio-errors previously observed with this class of catalysts were also detected (*17*). Importantly, the NMR spectra showed neither detectable vinylidene end-groups, which would arise from β-hydride elimination, nor peaks consistent with random ethylene-*co*-propylene segments; this confirms there is minimal tapering in the materials. Consistent with this reactivity, catalyst **1**/$B(C_6F_5)_3$ was capable of synthesizing PE/*i*PP tetrablock copolymers (entries 4 and 5). GPC analysis of aliquots taken after complete consumption of the monomers showed that molecular weights increased after each monomer addition and molar mass dispersities remained low (Fig. S3), although some molecular weight broadening was observed due to precipitation of the insoluble, semicrystalline polymer.

Table 1. Properties of PE/*i*PP block copolymers.[a]

Entry	Product (PP$_{kDa}$PE$_{kDa}$)	Cat. (μmol)	C_3H_6 (g)	$P_{ethylene}$ (atm)	t_{rxn} C_2H_4 (min)	Yield (g)	M_n (*theo.*) (kg/mol)	M_n (*tot.*) (kg/mol)	Đ (M_w/M_n)	T_m (°C)
1	PP$_{71}$PE$_{137}$	30	2.3	2.7	10	6.2	207	208	1.29	133
2	PP$_{73}$PE$_{50}$	30	2.3	2.7	5	3.9	130	123	1.29	131
3	PP$_{24}$PE$_{31}$	75	1.5	2.0	3	3.3	44	55	1.32	132
4	PP$_{36}$PE$_{20}$PP$_{34}$PE$_{24}$	25	1.0, 1.0	1.4, 1.4	4, 4	3.0	120	113	1.38	124
5	PP$_{60}$PE$_{80}$PP$_{75}$PE$_{90}$	30	2.0, 2.0	2.7, 2.7	4, 4	8.5	283	306	1.29	126

[a] See supplementary materials for experimental details.

Owing to thermodynamic incompatibility, weak van der Waals interactions, and the accumulation of amorphous polymer at the junction between melt molded laminates, most commercial grades of *i*PP and PE homopolymers display poor interfacial adhesion (*9*). We used a simple peel test to evaluate adhesion between heterogeneous grade PE and *i*PP laminates with and without the presence of the block copolymer as an adhesive layer (Fig. 2). Rectangular plaques of bilayer (PE/*i*PP) and trilayer (with block copolymer film) were compression molded in the melt and then pulled apart while monitoring the peel strength (*S*, force/sample width). This test provided a facile method for comparing the interfacial strength between the molded films. We report the results obtained from 100 μm thick block copolymer films, but note that no thickness dependence was observed down to 5 μm solvent cast films (Fig. S9).

Figure 2 shows representative peel test results obtained as a function of block copolymer molecular architecture and molecular weight. Laminates without block copolymer peel apart easily, ($S < 0.5$ N/mm). Incorporation of the $PP_{24}PE_{31}$ and $PP_{73}PE_{50}$ diblock copolymers increase the peel strength to $S \approx 1$ N/mm and $S \approx 3$ N/mm, respectively. Increasing the molecular weight of both blocks beyond a threshold value leads to a dramatic change in the failure mechanism from adhesive failure (low molecular weights) to cohesive failure (fracture, $S > 6$ N/mm) of the PE homopolymer film above about 75 kg/mol as shown in Fig. 2 (Fig. S4, S5). The interfacial strength between the diblock and homopolymer films is dependent on the block sizes due to two factors. The block copolymer acts as a surfactant, eliminating the thermodynamic driving force for amorphous materials to localize at the interface between block copolymer and *i*PP and PE film junctions (*9*). In some respects, the block copolymer acts as a type of macromolecular welding flux material. Secondly, increasing the overall block size enhances interpenetration and the number of entanglements between the chemically identical blocks and homopolymers chains in the melt state (*21, 22)*. Moreover, we anticipate a threshold molecular weight beyond which the polymer block will be able to bridge the amorphous layers associated with the lamellar morphology of semicrystalline polymers such as *i*PP and PE leading to co-crystallization along the film interfaces as shown in Fig. 2B and Fig. S15 (*21*). Lower molecular weight blocks are less capable of reaching the homopolymers crystalline lamellae (Fig. 2C) and will be prone to chain pull-out, resulting in lower adhesive strength. The welding effect was observed in various polyolefin materials (Fig. S7) and only with semi-crystalline block polymer adhesives (Fig. S8).
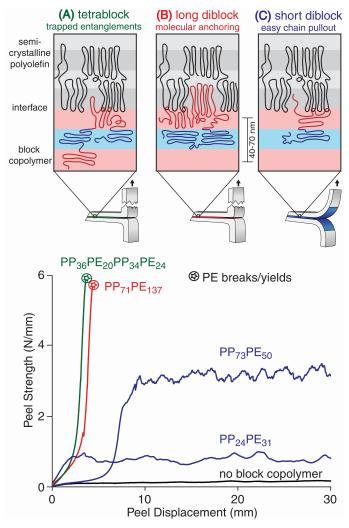
Fig. 2. Peel strength between commercial PE/*i*PP with various block copolymers.
Rectangular sheets (0.6 cm by 6 cm, 340 μm thick) of PE/*i*PP were laminated in the melt at 180 °C with and without PE/*i*PP block copolymer layers (100 μm thick) and pulled apart at 10 mm / min. Specimens were investigated with SEM imaging after testing (Fig. S6). Proposed models to explain adhesive differences of (**A**) tetrablock, (**B**) high M_n diblock and (**C**) low M_n diblock copolymers. Block copolymers are in multiple lamella (40-70 nm) (Fig. S17); first layer is shown. Stars indicate that PE films break or deform rather than undergo delamination.

The $PP_{36}PE_{20}PP_{34}PE_{24}$ tetrablock copolymer also exhibits extraordinary adhesive strength evidenced by cohesive failure (Fig. 2A), seemingly contradicting these arguments, as all the blocks are well below the threshold molecular weight required for cohesive failure with diblocks. We invoke a different mechanism for this result. A tetrablock molecular architecture ensures that half the iPP and PE blocks are flanked by the thermodynamically incompatible counterparts. This implies that interfacial mixing during melt compression produces entangled loops that effectively stitch together the homopolymers and block copolymer films upon crystallization when the laminates are cooled as illustrated in Fig. 2A. Similar arguments account for the enhanced toughness of bulk multiblock versus triblock polymers (*23, 24*). Consistent with this line of reasoning, the $PP_{36}PE_{20}PP_{34}PE_{24}$ tetrablock copolymer is microphase separated up to 260 °C as shown by rheological measurements (Fig. S17).

Challenges of recycling mixed polyolefin municipal waste (typically 70:30 PE:iPP) are in part due to interfacial phase separation leading to poor mechanical properties (*5-7*). Since specialty grades of PE and iPP can be blended to improve impact and crack resistance, the effective compatibilization of heterogeneous grade polyolefins may allow an upcycling of plastic wastes into higher value materials (*12*). Figure 3A shows the morphology obtained from a heterogeneous grade polyolefin blend containing 70 wt% PE and 30 wt% iPP and Fig. 3B illustrates the consequences of adding 5 wt% of tetrablock $PP_{60}PE_{80}PP_{75}PE_{90}$ to this mixture. Interfacial activity of the block copolymer is evidenced by a reduction in the average droplet size from 2.2 μm to 0.55 μm with the addition of the tetrablock copolymer; similar results were obtained with other architectures (Figs. S11-S14).

Individually, the pure iPP and PE display ductility and strain hardening when pulled in tension at room temperature (Fig. 3C). Blending the two components leads to a phase separated material and drastic reduction in strain at break ($\varepsilon_b = 12\%$ versus 300% and 800% for iPP and PE, respectively). Addition of 5 wt% $PP_{60}PE_{80}PP_{75}PE_{90}$ raises $\varepsilon_b = 600\%$, due to the combined effects of interfacial adhesion, reduced particle size, and efficient stress transfer between phases (Fig. S16). With just 1% of this tetrablock copolymer $\varepsilon_b = 450\%$, while addition of 1 wt% of the corresponding diblock copolymer, $PP_{60}PE_{80}$, which leads to a modest improvement, $\varepsilon_b = 90\%$. The low molecular weight tetrablock polymer $PP_{36}PE_{20}PP_{34}PE_{24}$ exhibited similar properties as did other PE:iPP ratios (Fig. S18).
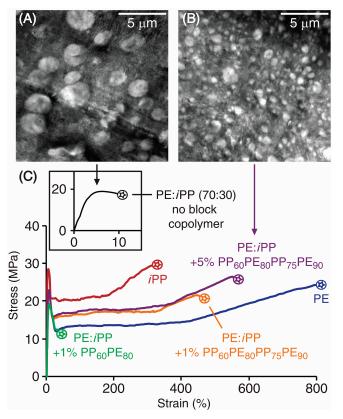
Fig. 3. Uniaxial tensile elongation of PE/*i*PP materials and blends. (**C**) Materials were melt blended at 190 °C without block copolymer (black) or with 1 wt% diblock (green), tetrablock (orange), or 5 wt% tetrablock (purple) then compression molded into tensile specimens at 180 °C, and strained at a rate of 100 %/min (Fig. S10). TEM images of PE/*i*PP blends show droplet morphology (**A**) without block copolymer and (**B**) with 5 wt% tetrablock copolymer.

In conclusion, we have developed a catalyst system capable of synthesizing semi-crystalline PE/*i*PP multiblock copolymers with precise control over block length and architecture. These macromolecules form strong interfaces with commercial PE and *i*PP when properly designed. Two molecular mechanisms are proposed to explain the molecular weight dependence of diblock copolymer adhesion and the behavior of tetrablock copolymers with relatively short blocks. The interfacial strength translates into control over morphology and mechanical toughness in melt blends of commercial PE and *i*PP, blends that are otherwise brittle at a ratio found in the municipal waste stream.

References and Notes:

1. D. B. Malpass, E. I. Band, "Introduction to Polymers of Propylene" in *Introduction to Industrial Polypropylene: Properties, Catalysis, Processes* (Scrivener, Beverly, MA, 2012), pp. 1–18.
2. M. Stürzel, S. Mihan, R. Mülhaupt, From Multisite Polymerization Catalysis to Sustainable Materials and All-Polyolefin Composites. *Chem. Rev.* **116**, 1398–1433 (2016).
3. W. Kaminsky, Ed., *Polyolefins: 50 Years After Ziegler and Natta I* (Advances in Polymer Science, Springer, New York, NY, 2013).

4. D. Nwabunma, T. Kyu, Eds., *Polyolefin Blends*. (Wiley, Hoboken, NJ, 2008).

5. The New Plastics Economy: Rethinking the Future of Plastics (Ellen MacArthur Foundation, 2016); available at https://www.ellenmacarthurfoundation.org/publications/the-new-plastics-economy-rethinking-the-future-of-plastics.

6. M. Chanda, S. K. Roy, Eds., *Plastics Fabrication and Recycling* (Plastics Engineering Series, Taylor & Francis, Boca Raton, FL, 2009), pp. 2-1–2-41.

7. M. Xanthos, Recycling of the #5 Polymer. *Science* **337**, 700–703 (2012).

8. L. Resconi, L. Cavallo, A. Fait, F. Piemontesi, Selectivity in Propene Polymerization with Metallocene Catalysts. *Chem. Rev.* **100**, 1253–1345 (2000).

9. K. A. Chaffin, J. S. Knutsen, P. Brant, F. S. Bates, High-Strength Welds in Metallocene Polypropylene/Polyethylene Laminates. *Science* **288**, 2187–2190 (2000).

10. G. J. Domski, J. M. Rose, G. W. Coates, A. D. Bolig, M. Brookhart, Living Alkene Polymerization: New Methods for the Precision Synthesis of Polyolefins. *Prog. Polym. Sci.* **32**, 30–92 (2007).

11. P. Hustad, Frontiers in Olefin Polymerization: Reinventing the World's Most Common Synthetic Polymers. *Science* **325**, 704–707 (2009).

12. J. W. Teh, A. Rudin, J. C. Keung, A Review of Polyethylene-Polypropylene Blends and Their Compatibilization. *Adv. Polym. Tech.* **13**, 1–23 (1994).

13. Y. Lin, V. Yakovleva, H. Chen, A. Hiltner, E. Baer, Comparison of Olefin Copolymers as Compatibilizers for Polypropylene and High-Density Polyethylene. *J. Appl. Poly. Sci.* **113**, 1945–1952 (2009).

14. A. Colbeaux, F. Fenouillot, J.-F. Gérard, M. Taha, H. Wautier, Compatibilization of a Polyolefin Blend through Covalent and Ionic Coupling of Grafted Polypropylene and Polyethylene. I. Rheological, Thermal, and Mechanical Properties. *J. Appl. Polym. Sci.* **95**, 312–320 (2005).

15. V. Busico, R. Cipullo, N. Friederichs, S. Ronca, M. Togrou, The First Molecularly Characterized Isotactic Polypropylene-*block*-Polyethylene Obtain via "Quasi-Living" Insertion Polymerization. *Macromolecules* **36**, 3806–3808 (2003).

16. V. Busico, *et al.* Block Copolymers of Highly Isotactic Polypropylene via Controlled Ziegler-Natta Polymerization. *Macromolecules* **37**, 8201–8203 (2004).

17. T. R. Boussie, *et al.* Nonconventional Catalysts for Isotactic Propene Polymerization in Solution Developed by Using High-Throughput-Screening Technologies. *Angew. Chem. Int. Ed.* **45**, 3278–3283 (2006).

18. D. J. Arriola, E. M. Carnahan, P. D. Hustad, R. L. Kuhlman, T. T. Wenzel, Catalytic Production of Olefin Block Copolymers via Chain Shuttling Polymerization. *Science* **312**, 714–719 (2006).

19. G. W. Coates, G. J. Domski. Patent WO 2008112133A2 (2008).

20. O. W. Webster, Living Polymerization Methods. *Science* **251**, 887–893 (1991).

21. J. J. Benkoski, P. Flores, E. J. Kramer, Diblock Copolymer Reinforced Interfaces between Amorphous Polystyrene and Semicrystalline Polyethylene. *Macromolecules* **36**, 3289–3302 (2003).

22. C. Laurens, C. Creton, L. Léger, Adhesion Promotion Mechanisms at Isotactic Polypropylene/Polyamide 6 Interfaces: Role of the Copolymer Architecture. *Macromolecules* **37**, 6814–6822 (2004).

23. A. Phatak, L. S. Lim, C. K. Reaves, F. S. Bates, Toughness of Glassy–Semicrystalline Multiblock Copolymer. *Macromolecules* **39**, 6221–6228 (2006).

24. F. S. Bates, *et al*. Multiblock Polymers: Panacea or Pandora's Box? *Science* **336**, 434–440 (2012).
25. R. A. Stapleton, et al. Bulky Aluminum Alkyl Scavengers in Olefin Polymerization with Group 4 Catalysts. *J. Am. Chem. Soc.* **125**, 9246–9247 (2003).
26. G. H. Fredrickson, F. S. Bates, Dynamics of Block Copolymers; Theory and Experiment. *Annual Rev. Mat. Sci*., **26**, 501–550 (1996).
27. F. S. Bates, G. H. Fredrickson, Block Copolymers–Designer Soft Materials. *Phys. Today.* **52**, 32–38 (1999).

Author Contributions:

G.W.C. conceived the project. G.W.C., J.M.E., R.D.G., and A.M.L. designed and conducted experiments related to polymer synthesis. J.M.E., J.X., and C.M.T. designed and conducted experiments related to adhesion and blends. G.W.C., A.M.L., C.W.M., and F.S.B. designed experiments and directed research. J.M.E., G.W.C., A.M.L., J.X., and F.S.B. wrote the manuscript. All authors commented on manuscript.

Supplementary Materials:
Materials and Methods
Figs. S1 to S18
References (*25-27*)